



# Designing the regularity of biodegradable copolyester for sustainable hot-melt adhesives: Adhesion, removability, and biodegradability

Kwang-Hyun Ryu<sup>a</sup>, Ji-Hyun Cho<sup>a</sup>, Hoon Kim<sup>b,c</sup>, Hyeon-Su Jo<sup>a</sup>, Jong-Ho Back<sup>b,\*</sup>, Hyun-Joong Kim<sup>a,b,\*</sup>

<sup>a</sup> Program in Environmental Materials Science, Department of Agriculture, Forestry, and Bioresources, Seoul National University, Seoul 08826, Republic of Korea

<sup>b</sup> Research Institute of Agriculture and Life Sciences, College of Agriculture and Life Sciences, Seoul National University, Seoul 08826, Republic of Korea

<sup>c</sup> Graphy Incorporation, Graphy R&D Center, Seoul, Republic of Korea

## ARTICLE INFO

### Keywords:

Hot-melt adhesive  
Sustainable adhesive  
Adhesive  
Biodegradable polymer  
Crystallization behavior  
Biodegradation in compost  
Enzymatic degradation

## ABSTRACT

Recent research has increased in eco-friendly hot-melt adhesives as alternatives to conventional commercial hot-melt adhesives. However, there have been limitations in terms of removability and biodegradability. This study addresses these issues by designing a novel molecular structure for a single polymer, resulting in a sustainable hot-melt adhesive that offers strong adhesion, clear removability, and high biodegradability without additional additives. By varying the ratio of alcohol monomers 1,4-butanediol (BD) and ethylene glycol (EG) during polymerization, we synthesized poly(butylene adipate-co-butylene terephthalate-co-ethylene adipate-co-ethylene terephthalate) (PBEAT) with four block segments. We increased the open time by reducing the regularity of the molecular structure, controlling crystallization behavior, and inhibiting polymer chain packing. This improvement in wettability with the adherend allowed us to achieve a lap shear adhesion strength of 3.18 MPa. Additionally, we proposed a debonding mechanism based on the correlation between the crystallization temperature ( $T_c$ ) block copolymer's and shear adhesion failure temperature (SAFT), demonstrating the removability of the prepared hot-melt adhesive. Finally, analyses of hydrolysis, enzymatic degradation, and biodegradation in compost confirmed that reduced crystallinity enhances biodegradability. PBE<sub>30</sub>AT, exhibiting the strongest adhesion strength, achieves complete degradation in compost within 20 days, faster than neat poly(butylene adipate-co-terephthalate) (PBAT). This research offers a novel and practical approach to enhancing the potential and expandability of sustainable adhesives by tailoring the molecular structure of the polymer.

## 1. Introduction

Adhesives are substances that bond two different substances together and have been used in a wide range of industrial field [1]. Due to their convenience and extensive versatility, they have been employed in simple labeling and packaging [1] as well as advanced sectors such as biomedical [2-4], electronics [5-7], automotive [8], and shipping [9]. The adhesive market is forecast to increase to \$93.3 billion by 2028 [10], with related research expected to be conducted extensively. However, since adhesives have been mostly petroleum-based or non-biodegradable, there has been growing recognition that environmental approaches are necessary. Consequently, there has been a growing focus on developing sustainable adhesives by designing their compositions to be bio-based or biodegradable materials [11-13].

Eco-friendly approaches to materials have evolved to include bio-based, biodegradable, and recyclable materials [14]. Likewise, studies on sustainable adhesives have been developed from these perspectives, such as renewable resources [15-20], degradable materials [21-24], and removable materials for recycling [25]. Shuai *et al.* proposed a bio-based adhesive for plywood applications using lignin and suggested that it could serve as a replacement for existing formaldehyde-based adhesives [26]. Hillmyer *et al.* proposed the synthesis of a triblock copolymer derived from lactide, a bio-based monomer and degradable material for degradable pressure-sensitive adhesives (PSAs) [27]. Leiza *et al.* proposed aqueous PSAs that can be rapidly removed from water via isosorbide-based monomers, which could facilitate the recycling of glass substrates, especially bottles [25].

Adhesives depend on several mechanisms to exhibit their adhesion,

\* Corresponding authors at: Research Institute of Agriculture and Life Sciences, College of Agriculture and Life Sciences, Seoul National University, Seoul 08826, Republic of Korea

E-mail addresses: [jback@umn.edu](mailto:jback@umn.edu) (J.-H. Back), [hjokim@snu.ac.kr](mailto:hjokim@snu.ac.kr) (H.-J. Kim).

<https://doi.org/10.1016/j.polymdegradstab.2024.111022>

Received 26 August 2024; Received in revised form 27 September 2024; Accepted 30 September 2024

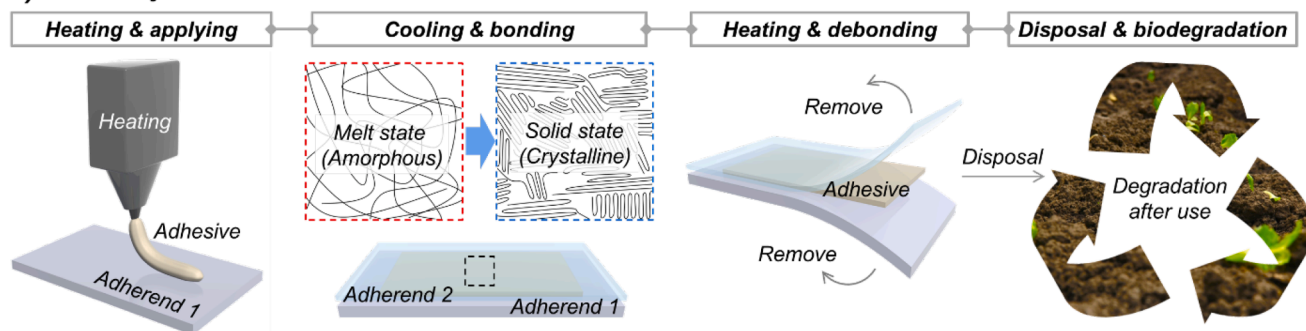
Available online 3 October 2024

0141-3910/© 2024 The Authors. Published by Elsevier Ltd. This is an open access article under the CC BY-NC-ND license (<http://creativecommons.org/licenses/by-nc-nd/4.0/>).

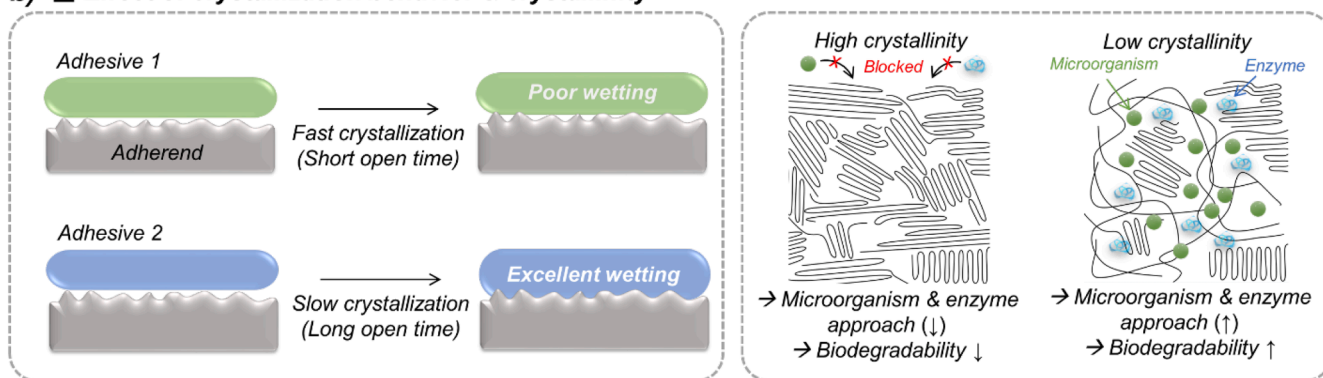
including curing induced by heat or light, pressure, and solvent evaporation [28]. Hot-melt adhesive (HMA) is a material composed of thermoplastic materials and exhibits adhesion when cooled after application by heating. The hot melt adhesives have various advantages, such as cost-effectiveness, absence of volatile organic compounds (VOCs) emissions, simplicity of working, long-term maintenance, and rapid setting [29]. The thermoplastic polymers typically used in hot melt adhesives are mainly polyolefin (PO) and ethylene vinyl acetate (EVA) [30]. In addition, hot melt adhesives are typically formulated by mixing these polymers with tackifiers, such as C5 resin, C9 resin, terpene resin, etc., and waxes [29]. However, these compositions are considered not to be eco-friendly in terms of being mainly petroleum-based sources,

negative impacts of biodegradation, and difficult to remove. The research on eco-friendly hot-melt adhesives was rare until a few years ago but has been increasing significantly recently. Bai et al. developed hot-melt adhesives by synthesizing poly(butylene-co-isosorbide succinate) using biomass-derived isosorbide monomers. Their study demonstrated that the adhesive strength improved with higher isosorbide content; however, they did not present conclusive evidence regarding the biodegradability of the adhesive [31]. Jin et al. proposed a method to prepare biodegradable hot-melt adhesives by copolymerizing poly(lactic acid) (PLA) and chlorinated poly(propylenecarbonate) using a chain extender. However, the biodegradability of the hot-melt adhesives were lower compared to that of neat PLA, and there was no additional

### a) Life cycle of sustainable hot-melt adhesives



### b) Effect of crystallization behavior & crystallinity



### c) Synthesis of PBEAT for sustainable hot-melt adhesives

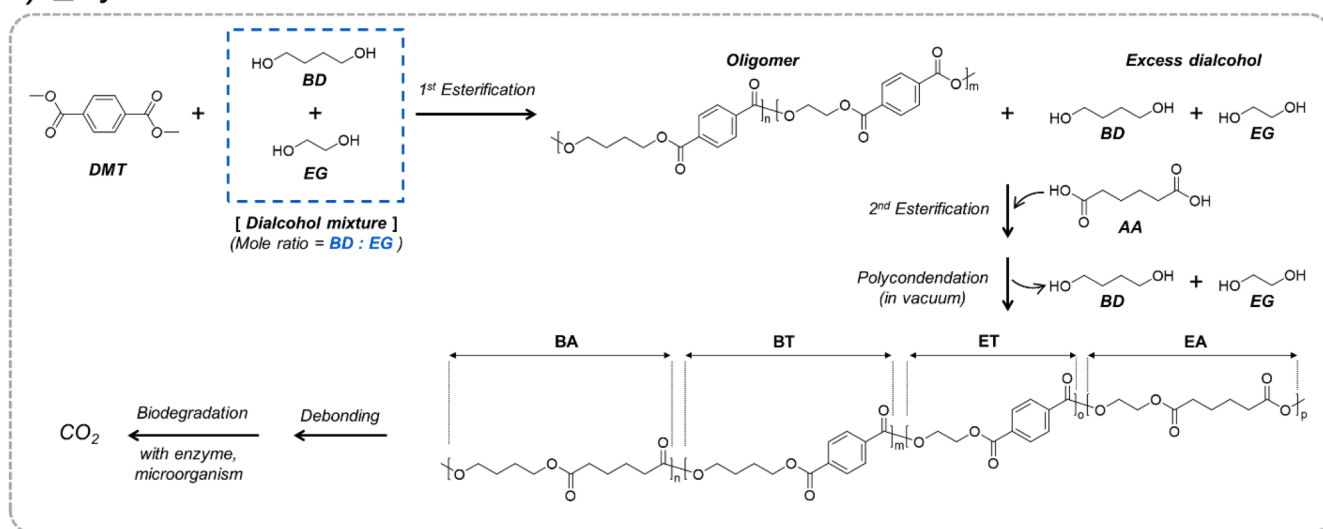


**Fig. 1.** (a) Scheme of sustainable hot-melt adhesives exhibiting bonding, removing, and biodegradation. (b) Design strategy for tailoring adhesion strength and biodegradability. (c) Synthesis process and chemical structure of PBEAT.

research addressing the removability [32]. Bao *et al.* proposed a chemically recyclable and reusable hot-melt adhesive utilizing supramolecular thermosetting polymers. However, the removal process required acidic conditions, and the material was not biodegradable [33]. Despite the growing research on eco-friendly hot-melt adhesives, significant limitations remain from an environmental perspective.

In this study, we devised a novel approach for preparing sustainable hot-melt adhesives, focusing on their desired adhesion strength, removability, and high biodegradability (Fig. 1a). In traditional hot-melt adhesives, tackifiers and waxes are added to increase adhesion, control crystallization behavior, and adjust viscosity [29]. In contrast, we designed the polymer without any additives to reduce the regularity of its structure, thereby tailoring its crystallization behavior and crystallinity for wettability and biodegradability. We selected block copolyester as a thermoplastic polymer to enable removability with the adherend after use for biodegradation. The clean deboned hot-melt adhesives were biodegradable, and the adherend without contamination by hot-melt adhesives was expected to be recyclable. Consequently, this approach enhanced the adhesion of biodegradable copolyester by tailoring the regularity of the polymer and can serve as a reference for further advancements in sustainable adhesives.

## 2. Experimental

### 2.1. Materials

Ethylene glycol (EG, > 99.5%, GR grade), 1,4-butanediol (BD, > 99.0%, GR grade), and adipic acid (AA, > 99.0%, GR grade) were purchased from Samchun Chemical Co., Ltd (Republic of Korea). Dimethyl terephthalate (DMT, ≥ 99.9%) was purchased from SK Chemical Co., Ltd (Republic of Korea). Tetrabutyl titanate (TBT, ≥ 97.0%, purum) as a catalyst was purchased from Sigma-Aldrich Co. LTD (USA). Lipase from *Aspergillus oryzae* (solution, ≥ 100,000 U/g, AR grade), phosphate buffer solution (Pbs, 10X, pH 7.4), and pure water (pH 5.0 - 8.0) were purchased from Sigma-Aldrich Co. LTD (USA), T&I Co. (Republic of Korea), and Samchun Chemical Co., Ltd (Republic of Korea), respectively. Standard compost was purchased from Abnexo Co., Ltd (Republic of Korea).

### 2.2. Synthesis of copolyester for hot-melt adhesives

The PBEAT polyesters were synthesized on a customized 3 L copolyester polymerization equipment divided into two reactors by polymerization in three steps: 1st esterification, 2nd esterification, and polycondensation (Figure S1). The mole ratio of DMT to AA in acid was fixed at 0.45:0.55, the mole ratio of EG to BD in alcohol according to each ratio, and the total mole ratio of acid to alcohol was set to 1:1.4. The total amount of acid monomers was 3 mol. and alcohol was 4.2 mol. The monomers and catalysts were added after purging the inside of the reactor with nitrogen. When adding the catalyst, it was always added together with a small amount of alcohol mixture. In the 1st esterification, DMT and the mixture of alcohol monomers, and 300 ppm of TBT were reacted with increasing temperature by 190 °C for 3 h until about 90% of methanol was removed as a byproduct. Then in the 2nd esterification, AA and 300 ppm of TBT were injected into the intermediate as oligomers. The reactants were reacted at 200 °C for 1 h until about 90% of water was removed as a byproduct. Lastly, 400 ppm of TBT was injected, and polycondensation was carried out at 230 °C in the bottom reactor. In order to appropriately eliminate excess alcohol monomers and byproducts, the vacuum was slowly lowered from atmospheric pressure to about 0.6 torr. The stirrer speed started at 105 rpm and the reaction was terminated when 90 rpm was reached, using a pole change motor. As a result, PBEAT polyester was obtained by discharging with pressurized nitrogen.

### 2.3. Structural analysis of copolyester

The number-average molecular weight ( $M_n$ ), weight average molecular weight ( $M_w$ ), and polydispersity index ( $PDI = M_w/M_n$ ) were characterized by gel permeation chromatography (GPC) with chloroform as an eluent. Three columns (two LF-804 and one LF-G, Resonac Corp.) and refractive index detector (RID-20A, Shimadzu Scientific Korea Corp.) were employed. The chamber temperature was fixed at 40 °C and the results were calibrated by polystyrene standard. The actual composition of the polymer was characterized by a high-resolution nuclear magnetic resonance spectrometer ( $^1\text{H NMR}$ , 600 MHz, AVANCE III HD, Bruker, Germany) with chloroform-d as a solvent. The crystallinity ( $X_c$ ) and crystal structure of the polymer were characterized by a diffractometer (WAXS, D8 DISCOVER, BRUKER, Germany) with a LYNXEYE XE detector. The wavelength of Cu- $\alpha$  radiation was 1.5418 Å, and X-ray emission power was fixed as 50 W with the angle varying from 3° to 40° (0.02° per step). The step was set to 0.02, and a single experiment was conducted to obtain XRD patterns of the copolyesters.

### 2.4. Thermal properties

The melting point temperature ( $T_m$ ), the crystallization temperature ( $T_c$ ), and the glass transition temperature ( $T_g$ ) of the copolyester were measured by differential scanning calorimetry (DSC, Q200, TA Instruments, USA). The samples ( $4.0 \pm 0.2$  mg) were heated to 200 °C from -10 °C with a fixed heating rate of 10 °C/min. These were cooled to -70 °C with a fixed cooling rate of -10 °C/min and then reheated to 200 °C with a fixed heating rate of 10 °C/min.  $T_{m1}$ ,  $T_{m2}$ ,  $\Delta H_{m1}$ ,  $\Delta H_{m2}$  were obtained from the 1st heating scan, the melt crystallization temperature ( $T_{mc}$ ) was obtained from 1st cooling scan, and  $T_g$ ,  $T_{m3}$ , and the cold crystallization temperature ( $T_{cc}$ ) were obtained from the 2nd heating scan. The shear adhesion failure temperature (SAFT) of the polymer was measured by using a holding power tester. The samples (2.5 mm x 2.5 mm x 0.3 mm) were placed on SUS304 and melted at 160 °C for 3 min, and corona-treated polyethylene terephthalate (PET) film was immediately attached (using a 2 kg roller, applied twice). The samples were stored at RT for 1 day. The samples were heated to 160 °C from room temperature (RT) with a heating rate of 0.5 °C/min, and SAFT was calculated by measuring the falling time of a 1 kg weight at 3 repetitions. The open time of the polymer was determined by heating the sample to 160 °C, allowing it to cool to RT, applying copy paper to the sample after a specified duration, and then peeling off the adherend to observe the failure mode (Figure S2).

### 2.5. Rheological properties

The shear storage modulus ( $G'$ ), shear loss modulus ( $G''$ ), complex viscosity ( $\eta^*$ ), and loss factor ( $G''/G'$ ) of the copolyester were measured using the modular compact rheometer (MCR 702e, Anton Paar GmbH, Austria). The following three steps were conducted to evaluate the application, wetting, crystallization, and debonding processes of the hot melt adhesive. In the first step, the sample was preheated to 160 °C for 5 min and then compressed by a measuring plate (diameter: 25 mm, gap: 1 mm). After trimming, the test was conducted at a fixed temperature of 160 °C over an angular frequency from 0.01 to 100 Hz at a shear strain of 5%. In the second step, the sample was cooled to 25 °C with a cooling rate of -10 °C/min, at a fixed angular frequency of 1 Hz and shear strain of 0.1%. Then, it was measured under isothermal conditions at 25 °C for 1 h, with the same angular frequency and shear strain. In the final step, the sample was precooled to -40 °C for 5 min, and heated to 160 °C with a heating rate of 5 °C/min, at a fixed angular frequency of 1 Hz and shear strain of 0.1%.

### 2.6. Adhesion of hot-melt adhesives

To evaluate the adhesion strength of the copolyester as a hot-melt

adhesive, we performed a single lap shear test using a steel or a stainless steel (SUS 304) substrate (**Figure S3**). Samples (25 mm x 25 mm x 0.3 mm) were prepared by melting the adhesive between two adherends. A spacer was used to ensure a uniform thickness and then stored at RT for 1 day. The excess residue was trimmed to maintain a consistent area and thickness and then measured using a universal testing machine (UTM, Z020, Zwick Roell Ltd, Germany) with a speed of 25 mm/min at 5 repetitions.

### 2.7. Biodegradation

To confirm the hydrolysis of the copolyester as a hot-melt adhesive, samples were immersed in pure water at RT (23 °C) and 58 °C, and the change in molecular weight was measured using GPC. To confirm degradability by enzymes, Pbs-based solution (Pbs: pure water = 5: 95 w/w) at a pH of 6.0 was mixed with lipase solution at a weight ratio of 100:1, and the prepared copolyester samples (15 mm x 15 mm x 0.1 mm) were immersed in the mixed solution. The mixed solution with lipase was then maintained at 58 °C, and the weight of the samples was measured after wiping the solution from the surface at 5 repetitions. To confirm biodegradability, the samples (50 mm x 50 mm x 0.1 mm) were buried in standard compost at 58 °C, and the weight of the samples was measured after gently wiping the compost from the surface at 5 repetitions. The relative humidity of the compost was maintained at 70–80%, while the pH was kept within a range of 5.0–6.5. A field-emission scanning electron microscope (SEM, SIGMA, Carl Zeiss AG, Germany) was used to observe the surface of samples after enzymatic degradation and biodegradation by compost.

## 3. Results and discussion

### 3.1. Design strategy

To develop a sustainable hot-melt adhesive, we selected PBAT as the primary biodegradable polymer. While other commercially used biodegradable polymers such as PLA, poly(butylene succinate) (PBS), poly(hydroxyalkanoates) (PHAs), and poly(caprolactone) (PCL) are available, each presents specific limitations for hot-melt adhesive applications [34–37]. For instance, PLA is brittle, PBS has high crystallinity leading to significant heat distortion, PHAs are cost-prohibitive, and PCL has a very low  $T_m$ , resulting in reduced thermal stability. Conversely, PBAT is characterized by low crystallinity, minimizing shrinkage issues, and possesses favorable viscoelastic properties due to its relatively low modulus. It is also highly ductile, allowing it to effectively absorb energy under external forces. Additionally, properties of PBAT can be easily tailored by conditioning with various acid and alcohol combinations. However, PBAT also crystallizes rapidly at RT and does not adequately wet the surface of the adherend, resulting in limited adhesion. This is due to the proportional relationship between shear strength and shear modulus; however, inadequate wetting restricts this relationship from effectively contributing to adhesion [38].

We hypothesized that reducing the regularity of the polymer could delay crystallization during cooling, thereby increasing the open time and allowing the hot-melt adhesive to adequately wet the adherend, ultimately enhancing adhesion (**Fig. 1b**). Furthermore, decreasing crystallinity of polymer is anticipated to facilitate the access of enzymes or microorganisms, thereby accelerating biodegradation. To modify the crystalline structure of PBAT, we performed esterification while increasing the mole fraction of EG, which contains two carbons less than BD (**Fig. 1c**). This approach was expected to introduce irregularity and hinder packing by increasing the number of repeating segments from the original two types in PBAT (butylene adipate (BA) and butylene terephthalate (BT)) to four types in PBEAT (BA, BT, ethylene adipate (EA), and ethylene terephthalate (ET)). Furthermore, it was hypothesized that using a block copolymer would enable debonding by selectively melting specific segments to reduce the modulus. Ultimately, we aimed to

develop a sustainable hot-melt adhesive that exhibits strong adhesive strength, allows for easy removal, and demonstrates high biodegradability.

### 3.2. Molecular structure of PBEAT

We synthesized copolyesters with reduced melt viscosity compared to conventional PBAT to utilize it as hot-melt adhesives without adding for additives (**Fig. 2a**, **Figure S4**). Since hot-melt adhesive becomes difficult to wet anymore once crystallization occurs after being applied to the adherend in a molten state, it is advantageous to have a low melt viscosity. To explore the effects of molecular structure irregularity, we ensured the viscosity of the polymerized samples was similar.

The peaks in the  $^1\text{H-NMR}$  spectra of the copolyester were assigned based on established references [39]. However, analysis of the chemical structure revealed significant peak overlap. This overlap was attributed to the relatively minor shift between BD and EG caused by the  $\beta$ -carbon (**Fig. 2b**). Despite this overlap, a distinct peak corresponding to each segment was identifiable, allowing for the determination of the mole fraction of each segment through assigned peak integration (**Figure S5**). The theoretical and experimental values showed similar mole fractions, confirming the successful synthesis of copolyesters with four block segments composed of BD and EG.

2D-WAXS analysis showed no distinct orientation but indicated a decrease in the crystalline area with increasing mole fraction of EG (**Fig. 2c**, **Figure S6**). Quantitative analysis revealed a significant reduction in  $X_c$  as the mole fraction of EG increased (**Fig. 2d**). This reduction might be attributed to decreased packing of polymer chain as the copolyester's segment number increased to four. Although the  $X_c$  increased in PEAT, this was likely due to improved chain packing facilitated by the segment number reverting to two. In addition, we found that the peak with a high crystalline area shifted as the mole fraction of EG increased, indicating that the  $d$ -spacing decreased (**Fig. 2e**). Furthermore,  $T_g$  in the amorphous region increased substantially with higher mole fraction of EG (**Figure S7**). This increase was attributed to lower conformational variability of EG and reduced free volume compared to BD. An increase in the mole fraction of EG in PBEAT resulted in an increased number of segments, reducing the molecular structure's regularity. This change resulted in decreased the  $X_c$  and flexibility of the polymer chains, which could slow the packing rate (**Fig. 2f**).

### 3.3. Adhesion

The crystallization temperature was assessed to verify the crystallization behavior associated with the copolyester segment (**Fig. 3a**). PBAT, known for its rapid crystallization, exhibited the highest  $T_{mc}$ . However, as the mole fraction of EG increased,  $T_{mc}$  progressively decreased. PBE<sub>30</sub>AT began to exhibit  $T_{cc}$ , indicating incomplete crystallization during the cooling process (**Figure S8**). Beyond PBE<sub>50</sub>AT,  $T_c$  was not measured, likely due to the significantly reduced crystallization rate.

To investigate the relationship between crystallization behavior and physical properties, rheometer measurements were conducted. The viscoelastic properties of the copolyester were measured to simulate the cooling process of a hot-melt adhesive. This method was conducted by sequentially measuring the cooling process at a rate of  $-10\text{ }^\circ\text{C}/\text{min}$  and the isothermal process at  $25\text{ }^\circ\text{C}$  (**Fig. 3b**). It was observed that samples with a high  $T_{mc}$  exhibited a rapid increase in  $G'$ , as indicated by the crossover point (where  $G' = G''$ ) during the cooling process (**Figure S9**). In contrast, for PBE<sub>30</sub>AT, the crossover point occurred at  $25\text{ }^\circ\text{C}$ , but it was confirmed that  $G'$  still remained around  $10^6\text{ Pa}$ , indicating the flowability of the adhesive. The peak of  $G''$  of this sample appeared over time at  $25\text{ }^\circ\text{C}$  and  $G'$  increased to about  $10^7\text{ Pa}$ . According to the Dalquist criterion, it is known that wetting into the adherend can occur when it is less than 1 MPa [40]. That is, it was verified that the time for the flowability of the sample to decrease was delayed as the mole fraction of

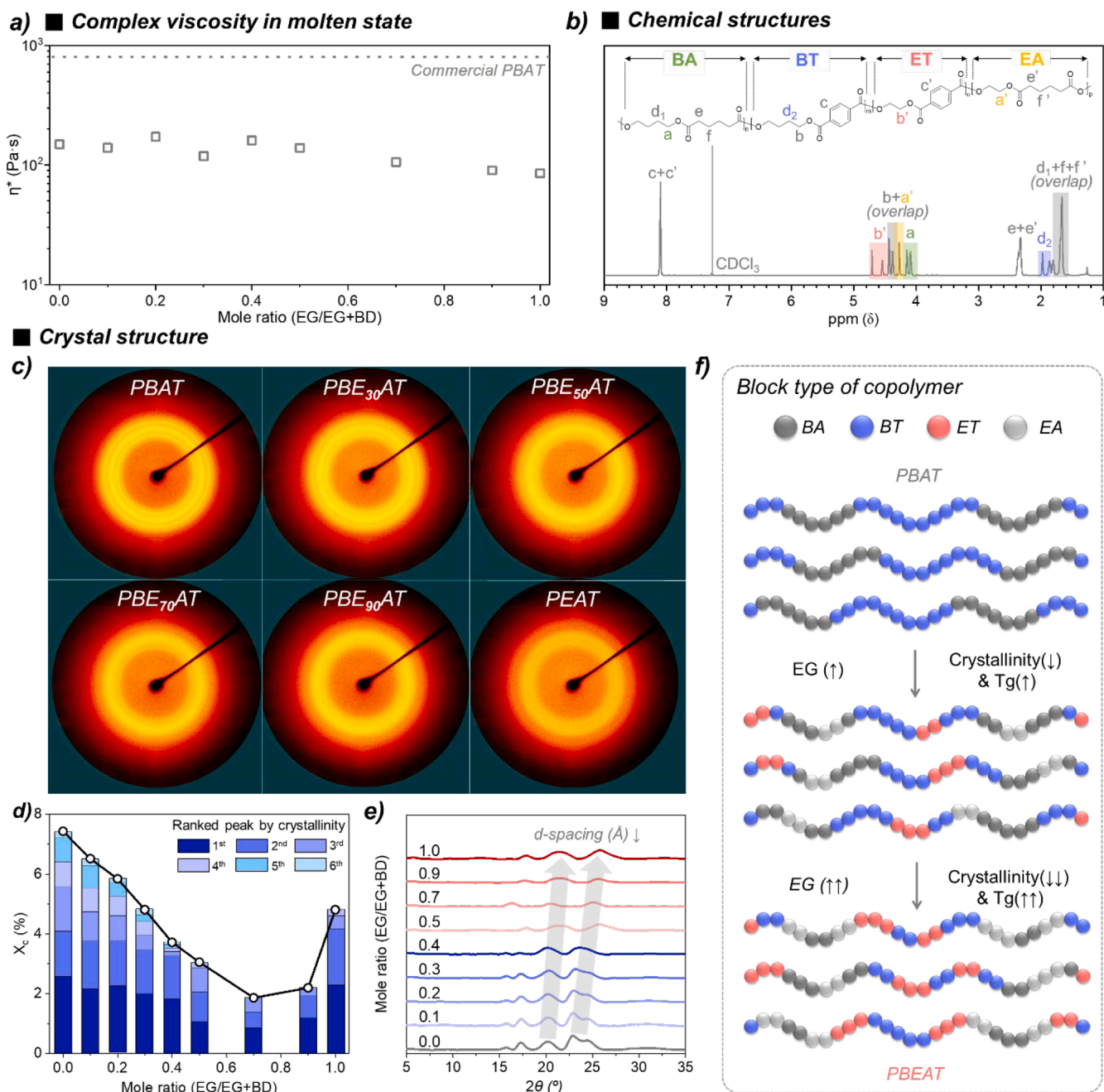


**Fig. 2.** a) Complex viscosity of the copolyester at 160 °C and angular frequency of 0.1 Hz. b) Chemical structure and  $^1\text{H NMR}$  spectrum of the PBE<sub>50</sub>AT. c) 2D-WAXS patterns of the copolyester. d) Crystallinity of copolyesters derived from WAXS results. e) WAXS patterns from the relative crystalline areas. f) Schematic illustrating the decrease in regularity of PBEAT with an increase in the mole fraction of EG.

EG increased (Fig. 3c). This trend was more clearly observed when measuring the open time, which was found to be consistent with the rheological results (Fig. 3d). This indicates that copolyesters with greater irregularity in their molecular structures require additional time for polymer chain packing, leading to an extended open time. We anticipated that the delay in open time would enhance the wettability of the prepared copolyesters, thereby improving their adhesion.

Given that shear strength is strongly influenced by the shear modulus [38], the  $G'$  of the copolyester at 23 °C was measured while heating from -40 °C to confirm this relationship (Fig. 3e). Up to PBE<sub>30</sub>AT, similar values of  $G'$  were observed; however, starting from PBE<sub>40</sub>AT,  $G'$  began to decrease significantly. This decline in  $G'$  is likely attributed not only to the substantial reduction in the  $X_c$  but also to the extended time required for crystallization in samples beyond PBE<sub>70</sub>AT, resulting in

even lower  $G'$  values.

Significant results were obtained when correlating the shear strength of the copolyester with its open time on a steel substrate (Fig. 3f). Despite showing similar  $G'$  up to PBE<sub>30</sub>AT, it was confirmed that the shear strength significantly increased and showed higher adhesion (3.18 MPa) than existing conventional hot-melt adhesives. It was reasonable that the micro-scale roughness of the adherend steel influenced adhesion strength, as increased wettability directly impacted bonding effectiveness (Figure S10). In other words, a longer open time likely provided more opportunity for wetting on the adherend surface, thereby creating a sufficient contact area. However, the shear strength decreased beyond PBE<sub>40</sub>AT, likely due to the observed reduction in  $G'$ . Furthermore, when comparing the lap shear strength on steel with SAFT results, the adhesive properties and thermal stability demonstrated were superior to

### Crystallization behavior

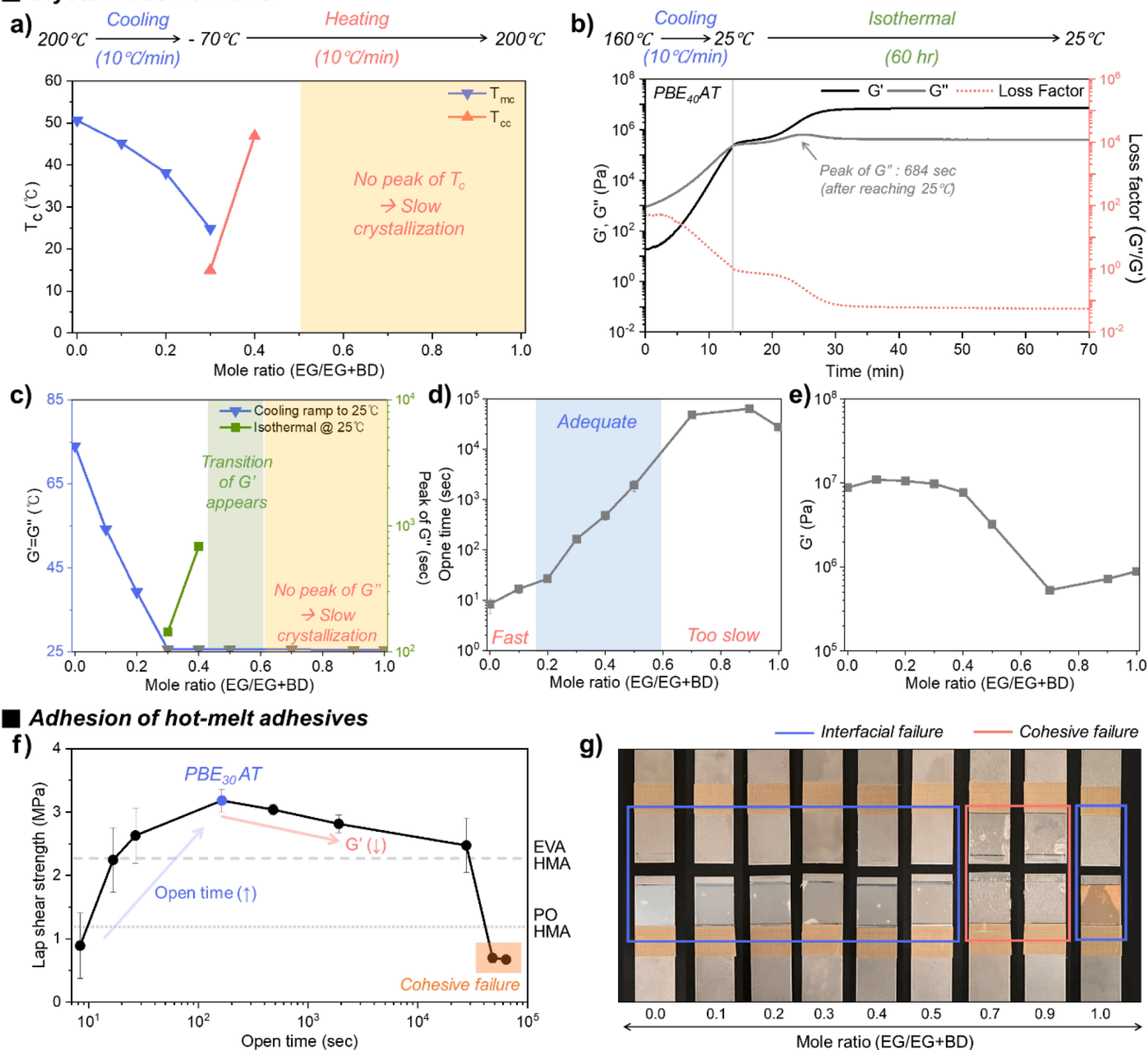


**Fig. 3.** (a) Crystallization temperature of the copolyesters by DSC. (b) Viscoelastic curve of PBE<sub>40</sub>AT and (c) viscoelastic properties of the copolyesters by simulating the cooling process of hot-melt adhesives. (d) Open time of the copolyester at RT. (e) Shear storage modulus of the copolyesters at RT and an angular frequency of 1 Hz. (f) Lap shear strength of the copolyesters on a steel substrate. (g) Failure mode of the copolyesters.

those of existing commercial products. (**Figure S11**). Interfacial failure was observed up to PBE<sub>50</sub>AT, which was attributed to the ductile nature of the copolyester (**Fig. 3g** and **Figure S12**). This characteristic suggests that the prepared copolyester in this study may be advantageous for debonding working. In contrast, commercial hot-melt adhesives were unsuitable for debonding, as they primarily exhibited cohesive or mixed failure (**Figure S13**). Notably, PEAT exhibited significantly higher shear strength and interfacial failure. As indicated by the open time results, PEAT requires more than 7 h to fully crystallize, suggesting a substantial difference in  $G'$  between the rheometer measurements and the shear strength tests. To investigate this, shear strength was measured 1 h after sample preparation, revealing a marked difference in adhesive strength (**Figure S14**). To assess the expandability of the prepared hot-melt adhesive, an adhesion evaluation was also carried out on a stainless steel substrate (**Figure S15**). Similar to the adhesion results on steel, it was observed that lap shear strength increased with longer open times.

However, the maximum adhesion appeared to decrease slightly, while the conventional HMA exhibited a slight increase. It was predicted that this would be influenced by the difference in surface energy of the substrate. Consequently, this study demonstrates that by controlling the regularity of the copolyester, wettability can be enhanced, making it suitable for use as a hot-melt adhesive.

### 3.4. Removability

The removability of the hot melt adhesives was verified by assessing the debonding working temperature and thermal stability through their viscoelastic behavior. Initially, we examined the changes in  $G'$  and  $G''$  at an angular frequency of 1 Hz while gradually increasing the temperature from -40 °C to 160 °C (**Figure S16**). It was observed that the crossover point (where  $G' = G''$ ) decreased as the mole fraction of EG increased. However, the crossover point occurring at  $T_g$  was excluded from the

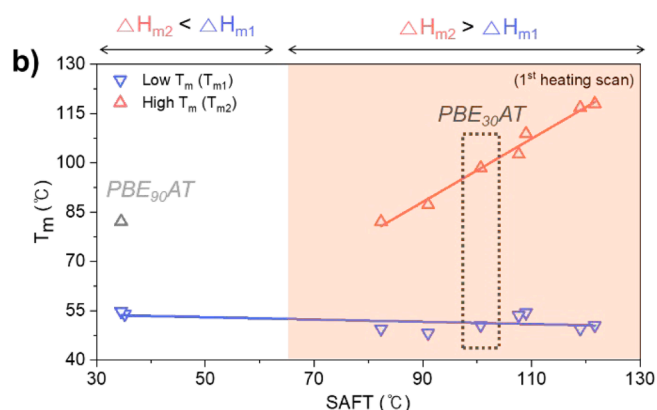
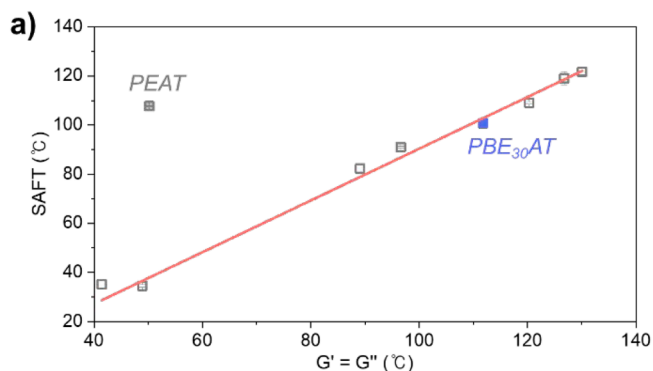
analysis, as it was not related to flowability (Figure S17). This viscoelastic change was directly linked to the thermal stability of the hot melt adhesives, as confirmed by correlating the data with the SAFT results (Fig. 4a). In other words, when heat was applied and the polymer became flowable, cohesion was lost, resulting in a complete loss of adhesive strength. Notably, PEAT exhibited significantly higher SAFT values, likely due to the increase in  $X_c$  observed after 1 day, as previously discussed.

Additionally, given that the prepared hot-melt adhesives consist of four block segments, there was a possibility of multiple  $T_m$ . To explore this,  $T_{m1}$  (the lower temperature  $T_m$ ) and  $T_{m2}$  (the higher temperature  $T_m$ ) were measured during the first heating without removing the heat history (Figure S18). While  $T_{m1}$  remained relatively stable,  $T_{m2}$  exhibited an initial decrease followed by an increase in mole fraction of EG, which corresponded to significant decrease in both the  $X_c$  as

determined by WAXS. Furthermore, correlating the  $T_m$  values obtained from the first heating cycle with the SAFT results confirmed that  $T_{m2}$  was associated with the thermal stability of the hot-melt adhesive (Fig. 4b). Notably, when  $\Delta H_{m2}$  was greater than  $\Delta H_{m1}$ , it was observed that the cohesion at elevated temperatures was dependent on  $T_{m2}$  (Figure S19). This suggests that, during debonding operation, the shear modulus could be reduced while still maintaining the cohesion of materials necessary to retain the shape of hot-melt adhesive.

In debonding operation, we identified two critical factors: 1) a significant reduction in adhesive strength, and 2) clean removal from the surface of adherend. The debonding test was conducted on PBE<sub>30</sub>AT to PBE<sub>50</sub>AT samples, which demonstrated higher adhesive strength compared to the conventional hot-melt adhesives. The debonding temperature was set to 10 °C lower than the SAFT results, where it does not completely melt. A significant decrease in  $G'$  was observed for the hot-

### Thermal stability for removability



### Removability of PBEAT

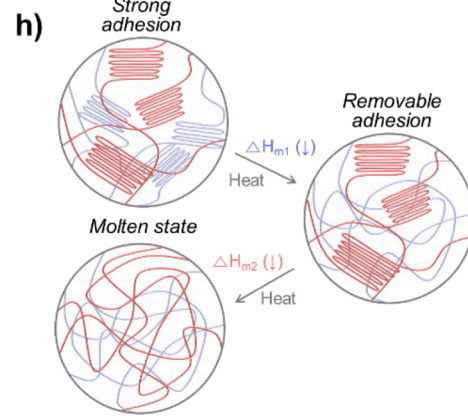
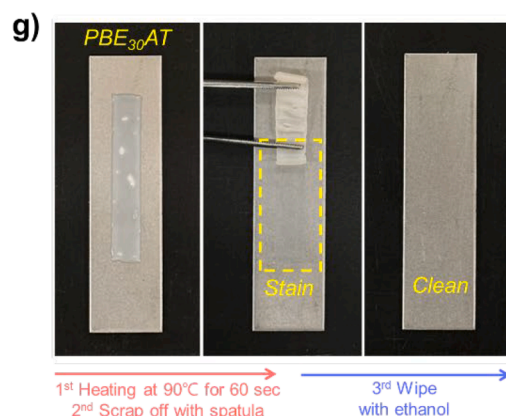
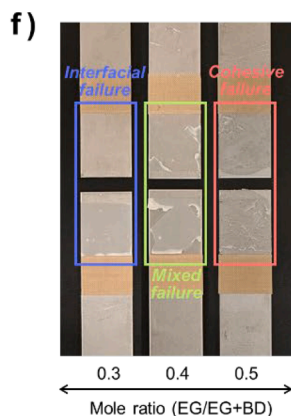
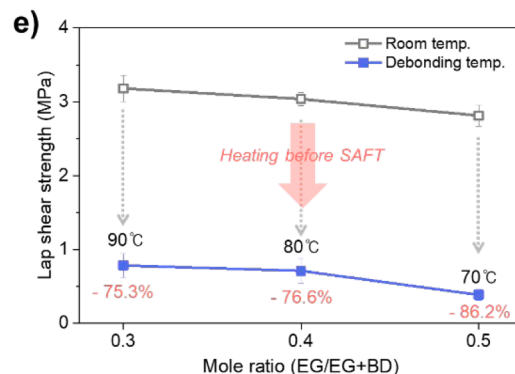
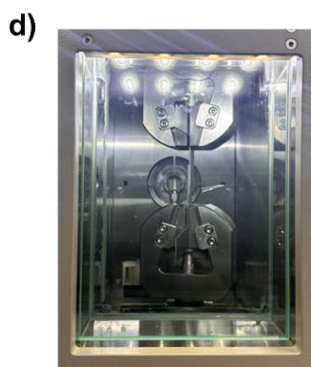
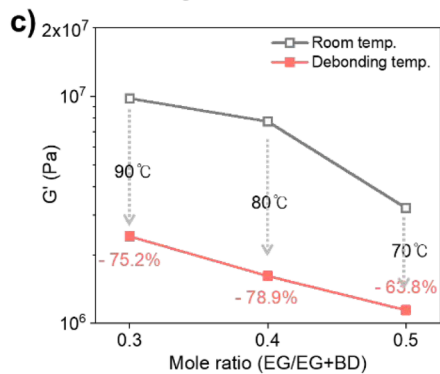
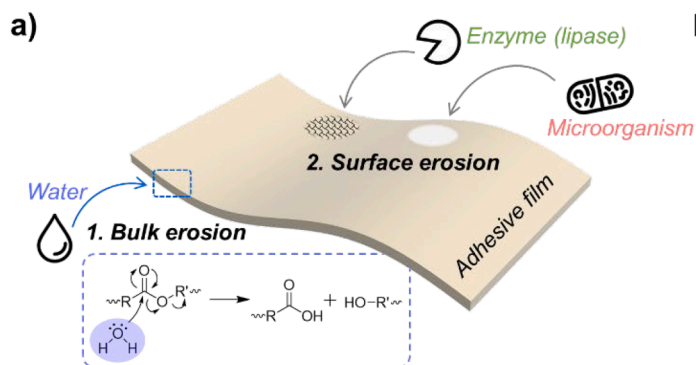


**Fig. 4.** (a) Correlation between SAFT and crossover point (where  $G' = G''$ ) during heating to 160 °C. (b) Correlation between SAFT and crystallization temperature. (c) Shear storage modulus of the copolyesters at debonding temperature and an angular frequency of 1 Hz. (d) Photo of chamber for debonding adhesion test. (e) Lap shear strength after heating at debonding temperature. (f) Failure mode of PBE<sub>30</sub>AT, PBE<sub>40</sub>AT, and PBE<sub>50</sub>AT. (g) Debonding operation process of PBE<sub>30</sub>AT. (h) Schematic representation of the debonding mechanism for the removable hot-melt adhesives.

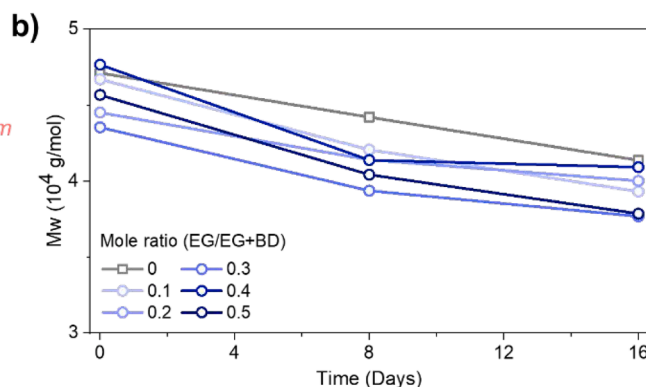
melt adhesives at this temperature (Fig. 4c). We hypothesized that adhesive strength could be reduced by selectively melting the crystal structure corresponding to  $\Delta H_{m1}$ , while maintaining the structure corresponding to  $\Delta H_{m2}$ . The removability test involved applying heat for 3 min in a chamber, followed by a lap shear test (Fig. 4d). A significant decrease in lap shear strength was confirmed across all samples (Fig. 4e), likely due to the substantial reduction in shear modulus as the

temperature increased. While PBE<sub>30</sub>AT and PBE<sub>40</sub>AT exhibited interfacial or mixed failure after lap shear test, respectively, PBE<sub>50</sub>AT displayed cohesive failure, making unsuitable for the intended purpose (Fig. 4f). Additionally, the prepared hot-melt adhesives were cleanly removed by scraping with a spatula after heating. In contrast, conventional hot-melt adhesives left sticky residue due to low cohesion under the same conditions (Fig. 4g and Figure S20). This clean removal was likely due to

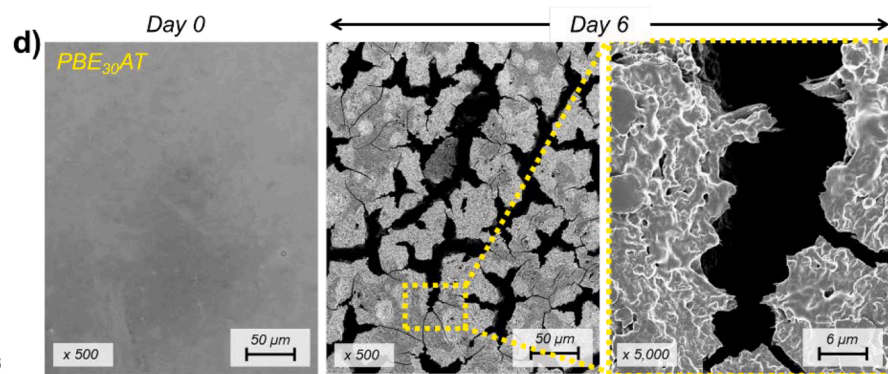
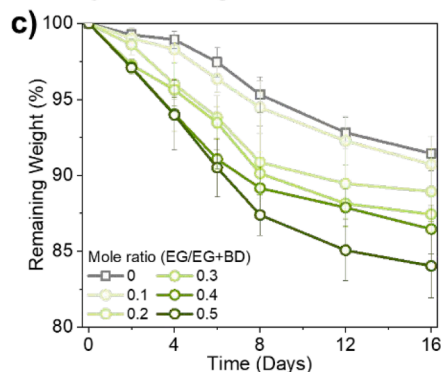
### Biodegradation mechanism



### Hydrolysis



### Enzymatic degradation



### Biodegradation in compost

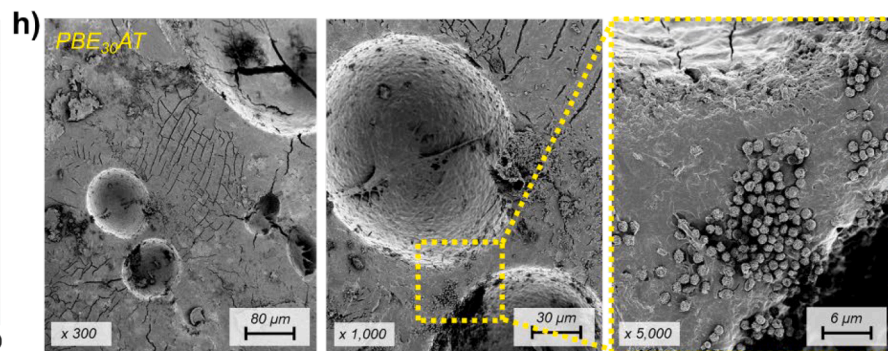
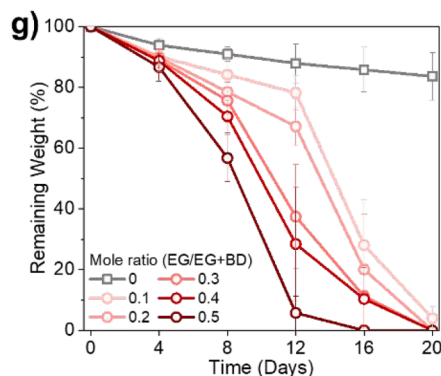


Fig. 5. (a) Schematic of biodegradation mechanism. (b) Molecular weight of the copolyester after hydrolysis at 58 °C. (c) Weight loss of the copolyester after enzymatic degradation at 58 °C. (d) Surface of PBE<sub>30</sub>AT observed by SEM after enzymatic degradation at 58 °C. (e) Photos of the PBE<sub>30</sub>AT degraded over time. (f) Photo of PBAT degraded after 16 days. (g) Weight loss of the copolyester after biodegradation in compost at 58 °C. (h) Surface of PBE<sub>30</sub>AT observed by SEM after biodegradation in compost at 58 °C.

the appropriate temperature-induced melting of the crystal structure corresponding to  $\Delta H_{m1}$ , while maintaining cohesion by preserving the structure associated with  $\Delta H_{m2}$  (Fig. 4h). If the hot-melt adhesive that was removed in this way was discarded and biodegraded, and the adherend was recycled, the developed copolyester was judged to be a novel sustainable hot-melt adhesive suitable for the purpose of this study.

### 3.5. Biodegradability

The biodegradation mechanism primarily consists of two steps: bulk erosion and surface erosion (Fig. 5a) [41]. Bulk erosion occurs when ester bonds within the polymer are randomly cleaved by water, leading to a decrease in molecular weight without significant weight loss. This process tends to accelerate with increasing temperature [42]. [43] Surface erosion, on the other hand, involves the cleavage of molecules from the surface by enzymes or microorganisms, resulting in weight loss. To better understand biodegradation in a composting environment at 58 °C, we conducted hydrolysis and enzymatic degradation tests. The samples tested ranged from PBAT to PBE<sub>50</sub>AT. Initially, hydrolysis results showed no significant decrease in molecular weight for samples soaked at RT for 16 days (Figure S21). However, at 58 °C, all samples exhibited a reduction in molecular weight by more than 90wt% (Fig. 5b). In hydrolysis results, no significant effect was observed concerning the mole fraction of EG.

In contrast, the presence of lipase led to the degradation of PBEAT, with a more rapid decrease of weight loss over time observed as the mole fraction of EG increased (Fig. 5c). This was likely due to the reduced crystallinity associated with a lower regularity of molecular structure, which makes it easier for lipase to cleave ester bonds. The surface of the sample degraded by lipase was confirmed through SEM as a result of degradation on the surface (Fig. 5d). Furthermore, in the absence of lipase, no weight loss or notable changes were observed, confirming that surface erosion of PBEAT occurs specifically in the presence of enzyme (Figure S22).

The results of the biodegradation test in the compost environment were particularly noteworthy. The prepared PBEAT-based hot-melt adhesives rapidly fragmented over time, leaving no trace in the compost (Fig. 5e). PBAT, known to have rapid biodegradability under 58 °C conditions [44], has demonstrated a slower rate of biodegradation than PBEAT (Fig. 5f). The trend in degradation rate to the mole fraction of EG was consistent with the enzymatic degradation test, showing significant weight loss in a short period (Fig. 5g). This rapid degradation in compost could be attributed to the combined effects of hydrolysis, enzymes, and microorganisms in compost (Figure S23). As a result of the SEM analysis, it was confirmed that the microorganisms found in the compost formed a cluster on the surface of the PBE<sub>30</sub>AT (Fig. 5h). These findings demonstrate that biodegradation can be accelerated by introducing irregularities into the molecular structure.

## 4. Conclusion

In this study, we aimed to address the limitations of existing hot-melt adhesives in terms of eco-friendliness. To achieve this, we developed a novel sustainable hot-melt adhesive that offers strong adhesive strength, removability, and biodegradability, all as a single polymer without the need for additional additives. PBAT was identified as the most suitable commercial biodegradable polymer; however, its rapid crystallization rate posed challenges for use as a single polymer. Therefore, we designed a modified polymer molecular structure.

By altering the mole ratios of EG and BD during copolyester polymerization, we transformed PBAT, originally consisting of two segments, into PBEAT, consisting of four segments. This modification not only significantly reduced crystallinity by decreasing the regularity of the polymer structure but also decreased chain mobility by increasing  $T_g$ . Additionally, we clearly demonstrated that the molecular structure

obtained and the associated crystallization behavior were directly related, leading to a significant increase in open time. As a result, we developed a hot-melt adhesive with a shear strength of 3.18 MPa in PBE<sub>30</sub>AT, surpassing the performance of existing conventional hot-melt adhesives. To ensure proper removability, the relationship between SAFT and  $T_m$  was confirmed, and it was found that there was a close relationship between  $T_{m2}$  and the cohesion of the hot-melt adhesive according to the temperature. This enabled effective adhering bonding and clean debonding, yielding significant results in terms of recyclability and biodegradability. We further analyzed hydrolysis, enzymatic degradation, and biodegradation in compost, focusing on bulk erosion and surface erosion as primary biodegradation mechanisms. With an increased mole fraction of EG, the  $X_c$  of PBEAT significantly decreased, facilitating enzyme and microorganism access. PBE<sub>30</sub>AT, which exhibited the strongest adhesion, achieved complete biodegradation within 20 days, a rate significantly faster than that of neat PBAT. When observing the surface of biodegraded samples by SEM analysis, very clear evidence of biodegradation was obtained. These novel hot-melt adhesives are expected to overcome the limitations of existing eco-friendly adhesives and advance the field of sustainable adhesives through obvious and detailed analysis.

### CRediT authorship contribution statement

**Kwang-Hyun Ryu:** Writing – original draft, Data curation, Conceptualization. **Ji-Hyun Cho:** Validation. **Hoon Kim:** Methodology. **Hyeon-Su Jo:** Methodology. **Jong-Ho Back:** Supervision, Conceptualization. **Hyun-Joong Kim:** Project administration, Funding acquisition.

### Declaration of competing interest

The authors declare the following financial interests/personal relationships which may be considered as potential competing interests:

Hyun-Joong Kim reports financial support was provided by Korea Ministry of Trade Industry and Energy. Kwang-Hyun Ryu reports financial support was provided by Korea Ministry of Trade Industry and Energy. Ji-Hyun Cho reports financial support was provided by Korea Ministry of Trade Industry and Energy. If there are other authors, they declare that they have no known competing financial interests or personal relationships that could have appeared to influence the work reported in this paper.

### Data availability

Data will be made available on request.

### Acknowledgment

This study was supported by the Technology Innovation Program (or Industrial Strategic Technology Development Program) (20009198, Development and Demonstration of Biodegradable Bioplastic Prototype) funded by the Ministry of Trade, Industry & Energy (MOTIE, Korea).

### Supplementary materials

Supplementary material associated with this article can be found, in the online version, at [doi:10.1016/j.polymdegradstab.2024.111022](https://doi.org/10.1016/j.polymdegradstab.2024.111022).

### References

- [1] D. Satas, *Handbook of Pressure Sensitive Adhesive Technology*, 3rd Ed., Satas & Associates, 1999.
- [2] G.M. Taboada, K. Yang, M.J.N. Pereira, S.S. Liu, Y. Hu, J.M. Karp, N. Artzi, Y. Lee, Overcoming the translational barriers of tissue adhesives, *Nature Reviews Materials* 5 (4) (2020) 310–329, <https://doi.org/10.1038/s41578-019-0171-7>.

- [3] D.M. Fitzgerald, Y.L. Colson, M.W. Grinstaff, Synthetic Pressure Sensitive Adhesives for Biomedical Applications, *Prog. Polym. Sci.* 142 (2023), <https://doi.org/10.1016/j.progpolymsci.2023.101692>. From NLM PubMed-not-MEDLINE.
- [4] S. Baik, H.J. Lee, D.W. Kim, J.W. Kim, Y. Lee, C. Pang, Bioinspired Adhesive Architectures: from Skin Patch to Integrated Bioelectronics, *Adv. Mater.* 31 (34) (2019) e1803309, <https://doi.org/10.1002/adma.201803309>. From NLM Medline.
- [5] W. Gao, H. Ota, D. Kiriya, K. Takei, A. Javey, Flexible Electronics toward Wearable Sensing, *Acc. Chem. Res.* 52 (3) (2019) 523–533, <https://doi.org/10.1021/acs.accounts.8b00500>. From NLM Medline.
- [6] T.R. Ray, J. Choi, A.J. Bandodkar, S. Krishnan, P. Gutruf, L. Tian, R. Ghaffari, J. A. Rogers, Bio-Integrated Wearable Systems: a Comprehensive Review, *Chem. Rev.* 119 (8) (2019) 5461–5533, <https://doi.org/10.1021/acs.chemrev.8b00573>. From NLM Medline.
- [7] J.H. Back, Y. Kwon, H. Cho, H. Lee, D. Ahn, H.J. Kim, Y. Yu, Y. Kim, W. Lee, M. S. Kwon, Visible-Light-Curable Acrylic Resins toward UV-Light-Blocking Adhesives for Foldable Displays, *Adv. Mater.* 35 (43) (2023) e2204776, <https://doi.org/10.1002/adma.202204776>. From NLM PubMed-not-MEDLINE.
- [8] M.D. Banea, M. Rosioara, R.J.C. Carbas, L.F.M. da Silva, Multi-material adhesive joints for automotive industry, *Composites Part B: Engineering* 151 (2018) 71–77, <https://doi.org/10.1016/j.compositesb.2018.06.009>.
- [9] S. Nam, Y.H. Yu, I. Choi, C.S. Bang, D.G. Lee, Fracture toughness improvement of polyurethane adhesive joints with chopped glass fibers at cryogenic temperatures, *Compos. Struct.* 107 (2014) 522–527, <https://doi.org/10.1016/j.compstruct.2013.08.015>.
- [10] Adhesives & Sealants Market Forecasts to 2028 - Global Analysis By Technology (Solvent-borne, Water-borne, Hot-melts, Reactive), End User (Electronics, Transportation, Healthcare, Building & Construction), and By Geography Statistics Market Research Consulting, 2022.
- [11] M.A. Hillmyer, W.B. Tolman, Aliphatic polyester block polymers: renewable, degradable, and sustainable, *Acc. Chem. Res.* 47 (8) (2014) 2390–2396, <https://doi.org/10.1021/ar500121d>. From NLM PubMed-not-MEDLINE.
- [12] M.A. Drosbecke, R. Aksakal, A. Simula, J.M. Asua, F.E. Du Prez, Biobased acrylic pressure-sensitive adhesives, *Prog. Polym. Sci.* 117 (2021), <https://doi.org/10.1016/j.progpolymsci.2021.101396>.
- [13] L.A. Heinrich, Future opportunities for bio-based adhesives – advantages beyond renewability, *Green Chemistry* 21 (8) (2019) 1866–1888, <https://doi.org/10.1039/c8gc03746a>.
- [14] J.G. Rosenboom, R. Langer, G. Traverso, Bioplastics for a circular economy, *Nat. Rev. Mater.* 7 (2) (2022) 117–137, <https://doi.org/10.1038/s41578-021-00407-8>. From NLM PubMed-not-MEDLINE.
- [15] G.S. Sulley, G.L. Gregory, T.T.D. Chen, L. Pena Carrodegua, G. Trott, A. Santmarti, K.Y. Lee, N.J. Terrill, C.K. Williams, Switchable Catalysis Improves the Properties of CO<sub>2</sub>-Derived Polymers: poly(cyclohexene carbonate-b-epsilon-decalonate-b-cyclohexene carbonate) Adhesives, Elastomers, and Toughened Plastics, *J. Am. Chem. Soc.* 142 (9) (2020) 4367–4378, <https://doi.org/10.1021/jacs.9b13106>. From NLM PubMed-not-MEDLINE.
- [16] A. Beharaj, I. Ekladios, M.W. Grinstaff, Poly(Alkyl Glycidate Carbonate)s as Degradable Pressure-Sensitive Adhesives, *Angew. Chem. Int. Ed. Engl.* 58 (5) (2019) 1407–1411, <https://doi.org/10.1002/anie.201811894>. From NLM PubMed-not-MEDLINE.
- [17] J.-H. Back, C. Hwang, D. Baek, D. Kim, Y. Yu, W. Lee, H.-J. Kim, Synthesis of urethane-modified aliphatic epoxy using a greenhouse gas for epoxy composites with tunable properties: toughened polymer, elastomer, and pressure-sensitive adhesive, *Composites Part B: Engineering* (2021) 222, <https://doi.org/10.1016/j.compositesb.2021.109058>.
- [18] S. Wang, L. Shuai, B. Saha, D.G. Vlachos, T.H. Epps 3rd, From Tree to Tape: direct Synthesis of Pressure Sensitive Adhesives from Depolymerized Raw Lignocellulosic Biomass, *ACS. Cent. Sci.* 4 (6) (2018) 701–708, <https://doi.org/10.1021/acscentsci.8b00140>. From NLM PubMed-not-MEDLINE.
- [19] H. Yang, X. Tan, G. Du, K. Ni, Y. Wu, Z. Li, X. Ran, W. Gao, J. Li, L. Yang, Development of biomass adhesives based on aminated cellulose and oxidized sucrose reinforced with epoxy functionalized wood interface, *Composites Part B: Engineering* 263 (2023), <https://doi.org/10.1016/j.compositesb.2023.110872>.
- [20] T. Jayaramudu, H.-U. Ko, H.C. Kim, J.W. Kim, E.S. Choi, J. Kim, Adhesion properties of poly(ethylene oxide)-lignin blend for nanocellulose composites, *Composites Part B: Engineering* 156 (2019) 43–50, <https://doi.org/10.1016/j.compositesb.2018.08.063>.
- [21] H. Jeong, S.-J. Hong, J.S. Yuk, H. Lee, H. Koo, S.H. Park, J. Shin, Renewable and Degradable Triblock Copolymers Produced via Metal-Free Polymerizations: from Low Sticky Pressure-Sensitive Adhesive to Soft Superelastomer, *ACS. Sustain. Chem. Eng.* 11 (12) (2023) 4871–4884, <https://doi.org/10.1021/acscuschemeng.3c00312>.
- [22] R. Abu Bakar, K.S. Hepburn, J.L. Keddie, P.J. Roth, Degradeable, Ultraviolet-Crosslinked Pressure-Sensitive Adhesives Made from Thioester-Functional Acrylate Copolymers, *Angew. Chem. Int. Ed. Engl.* 62 (34) (2023) e202307009, <https://doi.org/10.1002/anie.202307009>. From NLM PubMed-not-MEDLINE.
- [23] K.R. Albanese, Y. Okayama, P.T. Morris, M. Gerst, R. Gupta, J.C. Speros, C. J. Hawker, C. Choi, J.R. de Alaniz, C.M. Bates, Building Tunable Degradation into High-Performance Poly(acrylate) Pressure-Sensitive Adhesives, *ACS. Macro Lett.* 12 (6) (2023) 787–793, <https://doi.org/10.1021/acsmacrolett.3c00204>. From NLM PubMed-not-MEDLINE.
- [24] S.-J. Lee, G.-Y. Han, M.-B. Yi, J.-H. Back, H.-J. Kim, From waste to tape: inverse vulcanization of sulfur and solvent-based depolymerization for preparation of pressure-sensitive adhesives, *J. Mater. Res. Technol.* 29 (2024) 1798–1804, <https://doi.org/10.1016/j.jmrt.2024.01.218>.
- [25] A. Badia, A. Agirre, M.J. Barandiaran, J.R. Leiza, Removable Biobased Waterborne Pressure-Sensitive Adhesives Containing Mixtures of Isosorbide Methacrylate Monomers, *Biomacromolecules.* 21 (11) (2020) 4522–4531, <https://doi.org/10.1021/acs.biomac.0c00474>. From NLM Medline.
- [26] G. Yang, Z. Gong, X. Luo, L. Chen, L. Shuai, Bonding wood with uncondensed lignins as adhesives, *Nature* 621 (7979) (2023) 511–515, <https://doi.org/10.1038/s41586-023-06507-5>. From NLM Medline.
- [27] H.J. Kim, K. Jin, J. Shim, W. Dean, M.A. Hillmyer, C.J. Ellison, Sustainable Triblock Copolymers as Tunable and Degradable Pressure Sensitive Adhesives, *ACS. Sustain. Chem. Eng.* 8 (32) (2020) 12036–12044, <https://doi.org/10.1021/acscuschemeng.0c03158>.
- [28] A. Pizzi, K.L. Mittal (Eds.), *Handbook of Adhesive Technology*, 2nd Edition, 2003. Revised and Expanded.
- [29] S. Gharde, G. Sharma, B. Kandasubramanian, *Hot-Melt Adhesive: Fundamentals, Formulations, and Application: A Critical Review, Progress in Adhesion and Adhesives*, 2021.
- [30] J. Shields, *Adhesives Handbook*, Elsevier, 2013.
- [31] D. Qu, S. Sun, H. Gao, Y. Bai, Y. Tang, Biodegradable copolyester poly(butylene-co-isosorbide succinate) as hot-melt adhesives, *RSC. Adv.* 9 (20) (2019) 11476–11483, <https://doi.org/10.1039/c9ra01780a>. From NLM PubMed-not-MEDLINE.
- [32] J. Li, D. Wang, J. Jin, F. Li, Y. Gao, H. Liang, W. Jiang, Improving the Shear and Tack Strengths of Chlorinated Poly(propylene carbonate) through Chain Extension with Poly(lactic Acid) for Biodegradable Hot Melt Adhesives, *ACS. Appl. Polym. Mater.* 5 (12) (2023) 10256–10264, <https://doi.org/10.1021/acscapm.3c02029>.
- [33] C. Bao, Y. Yin, Y. Ding, J. Liu, Y. Xu, R. Miao, Z. Liu, B. Duan, Y. Qin, Z. Xin, Chemically Recyclable Supramolecular Thermosets toward Strong and Reusable Hot-Melt Adhesives, *Macromolecules.* 56 (17) (2023) 6633–6643, <https://doi.org/10.1021/acs.macromol.3c01063>.
- [34] A. Samir, F.H. Ashour, A.A.A. Hakim, M. Bassyouni, Recent advances in biodegradable polymers for sustainable applications, *Npj. Mater. Degrad.* 6 (1) (2022), <https://doi.org/10.1038/s41529-022-00277-7>.
- [35] K.W. Meereboer, M. Misra, A.K. Mohanty, Review of recent advances in the biodegradability of polyhydroxyalkanoate (PHA) bioplastics and their composites, *Green Chemistry* 22 (17) (2020) 5519–5558, <https://doi.org/10.1039/d0gc01647k>.
- [36] T.P. Haider, C. Volker, J. Kramm, K. Landfester, F.R. Wurm, Plastics of the Future? The Impact of Biodegradable Polymers on the Environment and on Society, *Angew. Chem. Int. Ed. Engl.* 58 (1) (2019) 50–62, <https://doi.org/10.1002/anie.201805766>. From NLM Medline.
- [37] Q. Ou-Yang, B. Guo, J. Xu, Preparation and Characterization of Poly(butylene succinate)/Poly(lactide) Blends for Fused Deposition Modeling 3D Printing, *ACS. Omega* 3 (10) (2018) 14309–14317, <https://doi.org/10.1021/acsomega.8b02549>. From NLM PubMed-not-MEDLINE.
- [38] J.B. Suh, A.N. Gent, I.S.G. Kelly, Shear of rubber tube springs, *Int. J. Non. Linear. Mech.* 42 (9) (2007) 1116–1126, <https://doi.org/10.1016/j.ijnonlinmec.2007.07.002>.
- [39] H. Kim, T. Kim, S. Choi, H. Jeon, D.X. Oh, J. Park, Y. Eom, S.Y. Hwang, J.M. Koo, Remarkable elasticity and enzymatic degradation of bio-based poly(butylene adipate-co-furanoate): replacing terephthalate, *Green Chemistry* 22 (22) (2020) 7778–7787, <https://doi.org/10.1039/d0gc01688h>.
- [40] W. Jo, K. Jeong, Y.-S. Park, J.-I.; Gap Lee, S. Im, T.-S. Kim, Thermally stable and soft pressure-sensitive adhesive for foldable electronics, *Chemical Engineering Journal* (2023) 452, <https://doi.org/10.1016/j.cej.2022.139050>.
- [41] B. Laycock, M. Nikolić, J.M. Colwell, E. Gauthier, P. Halley, S. Bottle, G. George, Lifetime prediction of biodegradable polymers, *Prog. Polym. Sci.* 71 (2017) 144–189, <https://doi.org/10.1016/j.progpolymsci.2017.02.004>.
- [42] R. Muthuraj, M. Misra, A.K. Mohanty, Hydrolytic degradation of biodegradable polyesters under simulated environmental conditions, *J. Appl. Polym. Sci.* (27) (2015) 132, <https://doi.org/10.1002/app.42189>.
- [43] M.A. Elsayy, K.-H. Kim, J.-W. Park, A. Deep, Hydrolytic degradation of polylactic acid (PLA) and its composites, *Renewable and Sustainable Energy Reviews* 79 (2017) 1346–1352, <https://doi.org/10.1016/j.rser.2017.05.143>.
- [44] P.D. Dissanayake, P.A. Withana, M.K. Sang, Y. Cho, J. Park, D.X. Oh, S.X. Chang, C. S.K. Lin, M.S. Bank, S.Y. Hwang, Effects of biodegradable poly(butylene adipate-co-terephthalate) and poly(lactic acid) plastic degradation on soil ecosystems, *Soil. Use Manage* 40 (2) (2024), <https://doi.org/10.1111/sum.13055>.